

UC San Diego

UC San Diego Previously Published Works

Title

Quantitative MS-based enzymology of caspases reveals distinct protein substrate specificities, hierarchies, and cellular roles

Permalink

<https://escholarship.org/uc/item/8rf639nt>

Journal

Proceedings of the National Academy of Sciences of the United States of America, 113(14)

ISSN

0027-8424

Authors

Tulien, Olivier

Zhuang, Min

Wiita, Arun P

et al.

Publication Date

2016-04-05

DOI

10.1073/pnas.1524900113

Peer reviewed

Quantitative MS-based enzymology of caspases reveals distinct protein substrate specificities, hierarchies, and cellular roles

Olivier Julien^a, Min Zhuang^{a,1}, Arun P. Wiita^{a,2}, Anthony J. O'Donoghue^{a,3}, Giselle M. Knudsen^a, Charles S. Craik^a, and James A. Wells^{a,4}

^aDepartment of Pharmaceutical Chemistry, University of California, San Francisco, CA, U.S.A. ¹Present address: School of Life Science and Technology, ShanghaiTech University, China. ²Present address: Department of Laboratory Medicine, University of California, San Francisco, CA, U.S.A. ³Present address: Skaggs School of Pharmacy and Pharmaceutical Sciences, University of California, San Diego, CA, U.S.A. ⁴Address correspondence to: jim.wells@ucsf.edu

Submitted to Proceedings of the National Academy of Sciences of the United States of America

Proteases constitute the largest enzyme family, yet their biological roles are obscured by our rudimentary understanding of their cellular substrates. There are twelve human caspases that play crucial roles in inflammation, cell differentiation and drive the terminal stages of cell death. Recent N-terminomics technologies have begun to enumerate the diverse substrates that individual caspases can cleave in complex cell lysates. It is clear that many caspases have shared substrates, however, little data exists about the catalytic efficiencies (k_{cat}/K_M) of these substrates, which is critical to understand their true substrate preferences. In this study, we use quantitative mass spectrometry to determine the catalytic efficiencies for hundreds of natural protease substrates in cellular lysate for two understudied members, caspases-2 and -6. Most substrates are new and the cleavage rates vary up to 500-fold. We compare the cleavage rates for common substrates to those found for caspases-3, -7 and -8 involved in apoptosis. There is little correlation in catalytic efficiencies among the five caspases suggesting each has a unique set of preferred substrates and thus more specialized roles than previously understood. We synthesized peptide substrates based on protein cleavage sites and found similar catalytic efficiencies between the protein and peptide substrates. These data suggest that the rates of proteolysis are dominated by local primary sequence and less by the tertiary protein fold. Our studies highlight that global quantitative rate analysis for post-translational modification enzymes in complex milieus for native substrates is critical to better define their functions and relative sequence of events.

N-terminomics | caspase | proteolysis | proteomics | apoptosis

Caspases are cysteine-class proteases that typically cleave after aspartic acid and play critical roles in cellular remodeling during development, cell differentiation, inflammation and cell death (reviewed in (1-3)). There are twelve caspases in humans alone which have been classically grouped based on sequence homology, domain architecture and cell biology as either inflammatory (caspases-1, -4, -5 and -11), apoptotic initiators (caspases-2, -8, -9 and -10) or executioners (caspases-3, -6, and -7) (4, 5). Identifying the natural protein substrates for caspases can provide important insights into their cellular roles. A series of large-scale proteomic studies from several labs have collectively identified nearly 2000 native proteins cleaved after an aspartic acid during apoptosis of human cells (recently reviewed in (6-8)). By adding individual caspases to extracts, it has been possible to begin to identify caspase-specific substrates ranging from just a few in the case of caspases-4, -5 and -9 (9), to several hundreds seen for caspases-1, -3, -7 and -8 (10, 11). Some of these substrates overlap, but others are unique to specific caspases. These substrate discovery experiments provide a useful starting point, but fail to address if a hierarchy exists for the cleavage events.

Kinetic studies have the potential to provide a much higher resolution picture by analyzing cleavage rates. For example, early

work measured the rates of cleavage for several purified protein substrates by caspase-3 and -7 showing significant rate differences (12). In another study, catalytic efficiency values (k_{cat}/K_M) were determined *in vitro* by quantitative SDS-PAGE for a sampling of eight purified caspase-3 substrates and found to vary 100-fold (from 10^4 to 10^6 M⁻¹s⁻¹) (13). A similar study of six caspase-1 substrates found them to vary in rate by about 200-fold, from 5×10^2 up to 1.2×10^5 M⁻¹s⁻¹ (9). Recently, quantitative mass spectrometry methods were applied to simultaneously calculate k_{cat}/K_M values for multiple substrates within cell extracts without the need to clone, express and purify the individual proteins (10). Seven-point rate curves were measured, which allowed calculation of k_{cat}/K_M values for 180, 58, and 66 substrates for caspase-3, -7 and -8, respectively. The rates of cleavage varied over 500-fold for each caspase. Together these studies began to suggest there is a strong hierarchy in the rates at which substrates in their natural milieu are cleaved by individual caspases.

Here, we apply discovery and quantitative MS-based proteomics to caspases-2 and -6 where there is far less known about their native substrates. Caspase-2 contains an initiator-like architecture with a long N-terminal caspase recruitment domain (CARD), yet it has a primary sequence preference for VDVAD (P5 to P1) (14), a motif that is more similar to the classical DEVD motif cleaved by executioner caspases-3 and -7. Caspase-6, on the other hand, has closest sequence homology and architecture to caspase-3 and -7, but is very inefficient at cleaving DEVD

Significance

Caspases, a family of twelve proteases involved in irreversible cell state changes including cell death, often cleave common substrates. However, we show by quantitative N-terminomics mass spectrometry, for caspases-2 and -6 that the rates of substrate cleavage vary over 500-fold in cellular lysate. The rates of cleavage show virtually no correlation among common substrates for these two, as well as three other caspases-3, -7 and -8. These global and unbiased studies reveal a greater degree of substrate hierarchy and specialized functions for caspases than previously appreciated. We believe this quantitative approach is of general use to other proteases and enzymes involved in post-translational modifications to better define their roles.

Reserved for Publication Footnotes

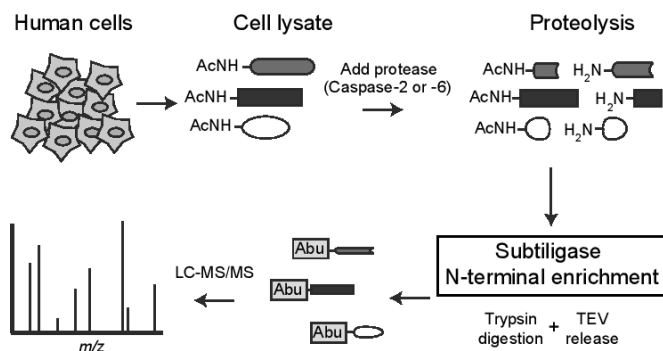


Fig. 1. Proteolytic substrate identification of caspase-2 and caspase-6 substrates using subtiligase-enrichment tagging technology. Schematic of the N-terminomics methodology employed for direct capture of proteolytic peptides. Jurkat cells are harvested and lysed. The α -amines of most proteins are naturally blocked by acetylation (AcNH-) unless there has been a proteolytic event (19). Endogenous proteases are pre-inactivated in the freshly prepared extract by addition of protease inhibitors, and excess thiol protease inhibitors are neutralized with dithiothreitol before addition of exogenous caspase. The engineered peptide ligase, subtiligase, is added together with a biotinylated ester (Fig. S2) to tag the free N-termini of endogenous proteins as well as the new N-termini generated by caspase proteolysis. The biotinylated proteins are captured using avidin beads, trypsinized and the N-terminal peptides subsequently released using TEV protease. This leaves behind a non-natural aminobutyric acid (Abu) residue that aids in identification. Substrate identification is performed using LC-MS/MS.

motifs and prefers hydrophobic residues at the P4 position, such as VEVD motifs seen for initiators. Caspase-6 has been implicated in neurodegenerative disease, including Huntington's and Alzheimer's diseases (15). Accordingly, finding small molecule modulators of caspase-6 are of great interest (16), and knowledge of the natural substrates could be useful for inhibitor and assay design.

Using the subtiligase-based N-terminomics technology in cell extracts (17), we discovered 235 and 871 protein substrates (with P1 = D) for caspase-2 and caspase-6, respectively. We were able to carry out quantitative kinetic studies in cell extracts and measured k_{cat}/K_M values for the top 49 and 276 individual substrates cut by caspase-2 and caspase-6, respectively. This allowed us to rank cleavage sites based on their roughly 500-fold variation in rate of proteolysis. The data when combined with quantitative proteomic data from caspases-3, -7, and -8 allowed us to make ten pair-wise comparisons among these five caspases, which showed virtually no correlation. These data strongly suggest that these caspases have very distinct cellular functions. Lastly, we find the catalytic efficiencies for the protein substrates are often comparable to linear peptides suggesting that primary sequence and not tertiary fold dominates cleavage rate and that native protein cleavage sites are as accessible as the linear peptides. Broadly, this work highlights the importance for quantitative proteomics of native proteins in complex mixtures to determine protein substrate specificity and to better understand the distinctive roles for proteases and other post-translational modifying enzymes.

Results

Discovery of caspase-2 and caspase-6 substrates in cell lysate reveals primary sequence specificity. As a source of extract, we used Jurkat cells, an immortalized line of human T lymphocyte cells (18). Although no single cell line expresses all proteins, Jurkat cells have been exhaustively used for studying apoptosis and more specifically, caspase function (3). Thus, Jurkat cells were our preferred cell line for making comparisons to published data. The protease activity for the exogenous caspase-2 and -6 was the same in buffer as compared to cell lysates suggesting the absence of endogenous inhibitors or activators in the cell lysate

(SI Appendix, Fig. S1). The subtiligase-based N-terminomics methodology (Fig. 1) was applied to recover cleaved products after addition of caspase-2 or -6. This attaches a biotin tag onto the α -amine of the cleaved N-terminal protein fragment. Virtually all labeling occurs at sites of either endogenous or exogenous proteolysis because >80% of natural N-termini for mammalian proteins are blocked by acetylation (AcNH-) during translation (19). The biotin labeled proteins are bound to avidin beads and trypsinized. The N-terminal peptide is released by cleaving the unique TEV protease cleavage sequence in the tag followed by identification by LC-MS/MS. The tagging and release process generates a non-natural remnant, aminobutyric acid (Abu), at the site of labeling which unambiguously confirms that the recovered peptide was labeled by subtiligase (SI Appendix, Fig. S2; see Materials and methods for details).

Caspases classically cleave their targets after an aspartic acid residue (P1 = D) (20). We found 277 aspartate cleavage sites in 235 proteins upon addition of caspase-2 (averaging 1.2 sites per protein), and 1120 cleavage sites in 871 putative caspase-6 substrate proteins (averaging 1.3 sites per protein) (Fig. 2A, Dataset S1 and Dataset S2). Over 70% of the cleavage sites were identified in two replicates (Fig. 2B) indicating good sampling coverage. The false discovery rates were <1.3% for both datasets at the peptide level and similar to our previous studies on other caspases. The majority of N-termini we observed (~4000 Abu tagged peptides) are derived from endogenous non-caspase endoproteolytic events, which we have previously observed in healthy cell extracts (3). In general, less than 3% of aspartic acid cleavage sites are detected in the absence of exogenous caspase suggesting little caspase activation. Several small-scale studies have previously identified a total of 37 and 68 substrates for caspases-2 and -6, respectively (11, 21, 22). More than half of the previously reported caspase-2 substrates were found in our dataset (19 out of the 37), while we identified 13 (out of 61) caspase-6 substrates reported in the CutDB database (<http://cutdb.burnham.org/>).

We compiled all the respective aspartate P1 recognition sequences of caspase-2 and caspase-6 (Fig. 2C) (23). The most prominent sequence cleaved by Caspase-2 is DEVD↓(G/S/A) that is remarkably similar to the consensus cleavage motif for the executioner caspases-3 and -7 (11). Our results did not show a strong specificity at the P5 position, with the possible exception of glutamate (SI Appendix, Fig. S3). Caspase-6 showed an initiator-like VEVD↓(G/S/A) consensus motif and only a faint preference for aspartate at P4, dissimilar to caspase-2, -3 and -7 at the P4 position. Interestingly, the caspase-6 data also showed a small enrichment for a negatively charged residue at P5 position. It is interesting to us that the consensus motifs for caspase-2 and -6 are more similar to executioner and initiator caspases, respectively, despite their domain architectures and homologies suggesting the opposite.

Bioinformatics analysis of caspase-2 and -6 substrates. We performed bioinformatics analysis of the 276 and 871 caspase-2 and -6 substrates identified in cell lysate, respectively. We observed virtually identical substrate cellular localization patterns for both datasets, with 35% of the substrates annotated as found in the cytoplasm, 37% in the nucleus, 5% in the endoplasmic reticulum, 6% at the cell membrane, 3% in the mitochondria, 2% are secreted proteins, while 12% are found in other organelles (or unknown) (SI Appendix, Fig. S4). This distribution is very similar to the distribution of substrates seen when we have induced apoptosis in intact cells (3). Moreover, the distribution is similar to the subcellular localization of all proteins found in the human proteome with the exception of secreted and cell membrane proteins, which are typically under-represented in proteomic experiments based on their extraction efficiency in whole cell lysates. Thus, the distribution of substrates is not biased by subcellular location for either caspases-2 and -6.

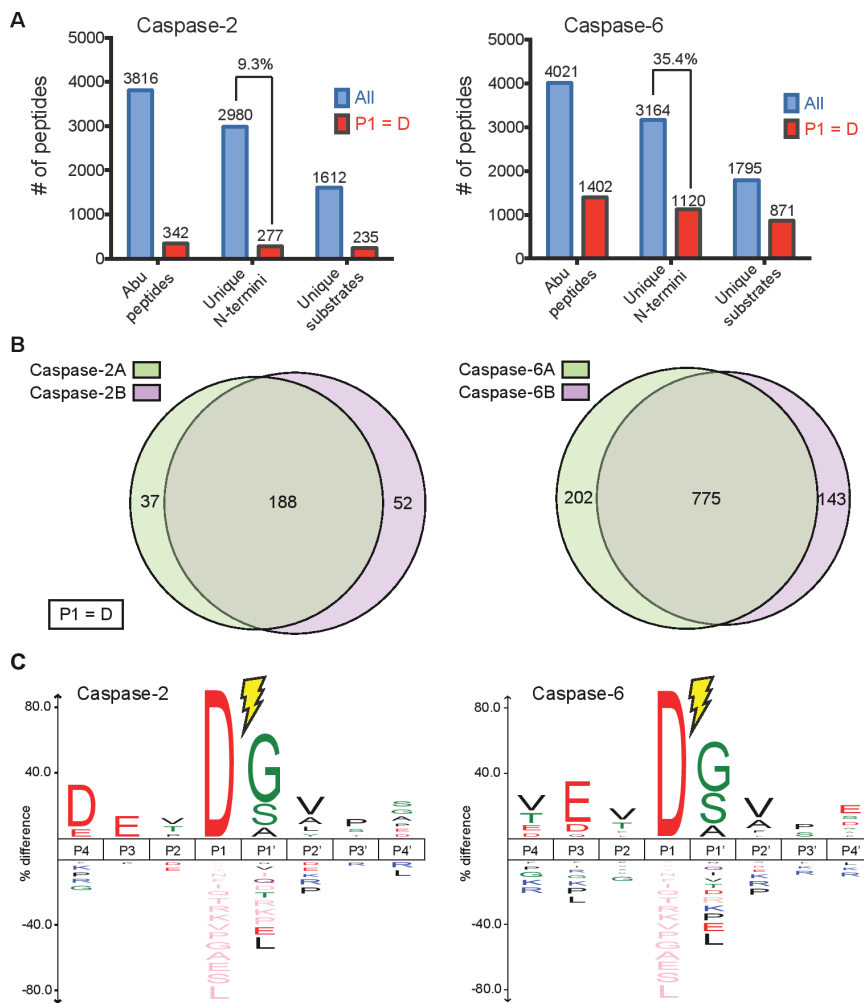


Fig. 2. Discovery of caspase-2 and caspase-6 substrates in cell lysates. A. Shown are the total number of unique peptides (tagged with Abu), unique cleavage sites and unique substrates at the protein level identified for caspase-2 (left) and caspase-6 (right). The subset of identifications featuring an Asp at P1 position is shown in red. Total peptides are colored in blue, while peptides originating only from a caspase cleavage event (aspartate at P1 position) are colored in red. B. The discovery experiments show greater than 70% overlap between the two biological replicates in the cleavage sites identified for both caspase-2 and caspase-6. C. Sequence recognition motifs of caspase cleavages for caspase-2 and caspase-6 shows highest consensus $\text{DEVD} \downarrow (\text{G/S/A})$ and $\text{VEVD} \downarrow (\text{G/S/A})$ motifs, respectively, (P value = 0.05). Consensus sequences were generated using iceLogo (23).

To obtain a general overview of caspase-2 and -6 biology, we performed a gene ontology enrichment analysis on both datasets (SI Appendix, Fig. S4, Dataset S3 and Dataset S4). For caspase-2, we found an enrichment for RNA processing, regulation of cell death, intracellular transport, chromosome organization and cytoskeleton. For caspase-6, we found enrichment for regulation of transcription, cell cycle, cell death, RNA splicing, cytoskeleton and response to DNA damage. Examples of substrates for each category are shown in SI Appendix Fig. S4.

Quantitative measurement of caspase-cleaved substrates using Selected Reaction Monitoring (SRM). In order to determine the rates of proteolysis of the natural protein substrates, we developed a scheduled selected reaction monitoring (SRM) method on a triple-quadrupole mass spectrometer (SI Appendix, Fig. S5). The 342 and 1402 aspartate-cleaved peptides identified for caspase-2 and -6, respectively, were evaluated for their suitability for SRM analysis. Using the sample from the discovery experiment (Fig. 2), SRM training data were acquired on a QTRAP 5500 LC-MS/MS to identify suitable peptides. Peptide transitions, known as precursor and product ion pairs, were chosen from the top seven most intense transitions and were searched within a 15 min retention time window. We selected only peptides showing four strong and unambiguous transitions, which ultimately led us to monitor 152 and 471 peptides (plus a control) for caspases-2 and -6, respectively. As above, we added caspase-2 and -6 to pre-neutralized cell lysate and quenched the caspases using the pan caspase inhibitor zVAD-fmk at each of seven time points

(0, 5, 15, 30, 60, 120, 240 min) before N-terminal enrichment and LC-MS/MS quantification. The appearance of each proteolytic substrate was monitored as a function of time (Fig. 3A). Using pseudo-first order kinetics, we performed automated non-linear fitting to determine the catalytic efficiency (k_{cat}/K_M) of each caspase substrate (Fig. 3B, Dataset S5 and Dataset S6). In total, we were able to measure 49 and 276 k_{cat}/K_M values for caspase-2 and -6, respectively. These values ranged two to four log units for caspase-2 and caspase-6, respectively (Fig. 3D). Most progress curves were monotonic and parabolic allowing calculation of k_{cat}/K_M values. The fastest substrates were cleaved at a rate of up to $10^5 \text{ M}^{-1} \text{ s}^{-1}$ (Fig. 3C-D; SI Appendix, Fig. S6), which rivaled several optimized synthetic fluorescent substrates (24-26). However, the catalytic efficiency values for the slowest ($<10^2 \text{ M}^{-1} \text{ s}^{-1}$) and fastest ($>10^5 \text{ M}^{-1} \text{ s}^{-1}$) reactions are less reliable than the intermediate cleavage reactions; the slowest reactions did not go to completion within the 240 minute assay time, while the fastest reactions were generally complete by the second time-interval (15 minutes) so only one or two data points could be fit. In future studies, various enzyme concentrations could be used to determine more accurately the proteolysis of these few substrates."

Western blots. Quantitation of cleavage rates for hundreds of substrates by immunoblot is impractical given the lack of suitable antibodies and prohibitive cost. Nonetheless, we chose to monitor the rates and extents of cleavage for two caspase-6 targets, the new substrate tuberous sclerosis 1 protein homolog (TSC1

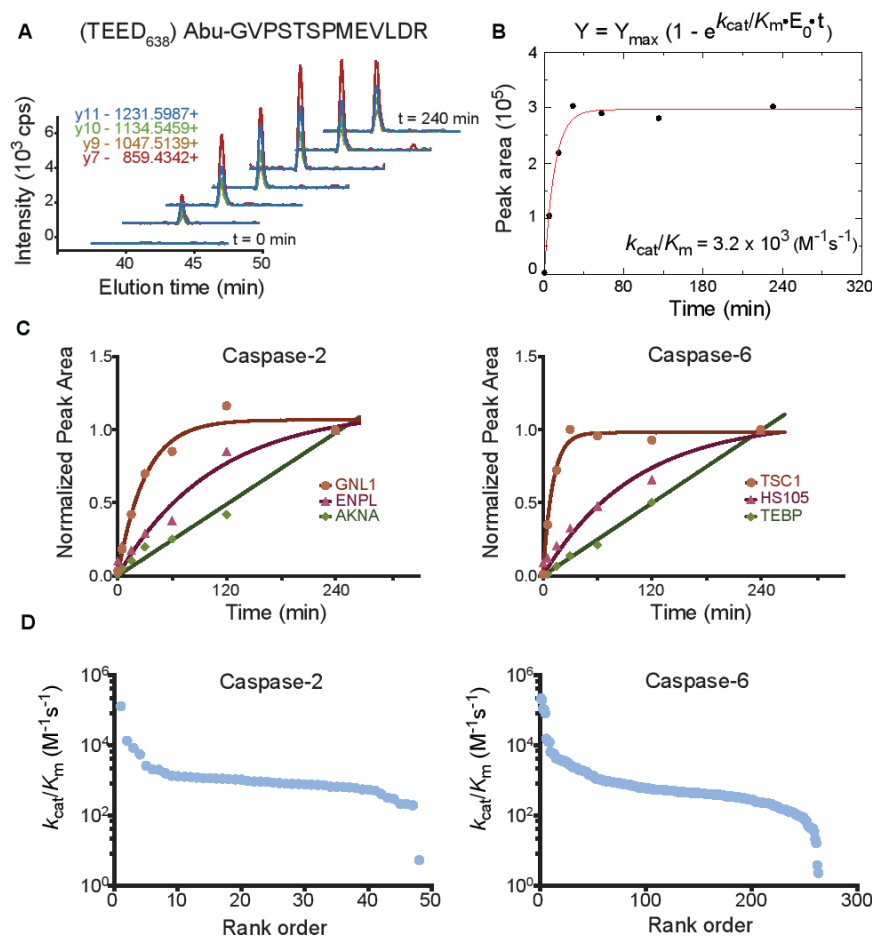


Fig. 3. Determination of catalytic efficiency values (k_{cat}/K_M) for caspase-2 and caspase-6 substrates using selected reaction monitoring (SRM). A. Example chromatograms of the four transitions monitored for a peptide from the TSC1 protein shows accumulation of cleavage product over time. B. The peak integrations were summed over the four transitions monitored to estimate extent of cleavage product and plotted as a function of time to determine the progress rate curve. C. The assays were analyzed using pseudo-first order kinetic conditions, and k_{cat}/K_M values were calculated as described in the methods for 49 and 276 cleavage sites for caspase-2 and -6, respectively. Three examples are shown for caspase-2 (left) and caspase-6 (right). D. A wide range of k_{cat}/K_M values were observed over two to four logs for caspase-2 and caspase-6 substrates, respectively. The fastest protein substrates ($10^5 \text{ M}^{-1} \text{ s}^{-1}$) can only be estimated because they saturated too rapidly. Most of the substrates are in the range $10^3 \text{ M}^{-1} \text{ s}^{-1}$ of which fit well because multiple points were obtained before saturation.

or hamartin), and the classic substrate poly [ADP-ribose] polymerase 1 (PARP1), for which suitable antibodies were available. We performed the same time course in extracts as done for the SRM analysis and monitored the disappearance of the full-length proteins and appearance of the cleaved products using traditional Western blotting (SI Appendix, Fig. S7). Full-length hamartin showed a marked reduction in intensity over time with simultaneous increase of cleaved product, consistent with cleavage at position 638 identified in the discovery experiment. Full length PARP1 showed similar results, with a decrease in the full-length protein and increase of the cleaved product, while the intensity of the GAPDH loading control remained unchanged. The rate constants obtained by Western blot analysis were within five-fold of those obtained by mass spectrometry for these two substrates; TSC1 (WB: 7.1×10^2 and SRM: $3.2 \times 10^3 \text{ M}^{-1} \text{ s}^{-1}$) and PARP1 (WB: 1.1×10^2 , SRM: $1.5 \times 10^2 \text{ M}^{-1} \text{ s}^{-1}$). The small discrepancies in rate constants are likely due to inherent variability and sensitivity between the two methods.

Pair-wise comparisons of rates for common substrates cleaved by caspases-2, -3, -6, -7 and -8 show virtually no correlation and highlight their unique substrate preferences. We performed a pairwise comparison of the rates of proteolysis obtained for identical cleavage sites that were shared between the caspases, comparing caspase-2 and -6 SRM data obtained here with values obtained for caspases-3, -7 and -8 previously from our laboratory (10). The number of common substrate sites shared between the two caspases ranged from as few as three (between caspases-2 and -8) to as many as 46 (between caspases-3 and -7) (Fig. 4A). We found virtually no correlation among the rates

at which these common substrates were cleaved (Fig. 4B-F and Dataset S7). This is true for all ten pair-wise comparisons. The only small connection observed among the five caspases studied is a weak anti-correlation between caspase-2 and -6 substrates. This suggests that individual caspases have preferred protein substrates and thus specific roles. This quantitative difference is not evident when looking at consensus cleavage motifs. For example, caspase-2, -3 and -7 show a consensus DEVD sequence motif in cell lysates, but the common substrates are cleaved at very different rates (Fig. 4B, 4C, 4E).

Comparisons of sequence cleavage patterns for protein and peptide substrates. We wished to assess whether the intrinsic rate and specificity toward linear substrate motifs differs among the caspases, and thus sought a peptide-library approach that would remove the influence of protein structure. An unbiased approach for characterizing linear peptide specificity of proteases, called multiplex substrate profiling by mass spectrometry (MSP-MS), has been applied to characterizing protease cleavage patterns (27). This *in vitro* technique uses a highly diversified tetradecapeptide library designed to present virtually all possible pairwise amino acid combinations at a minimum two-fold redundancy within a five position linear motif to a peptidase of interest (currently designed with 228 unique peptides). We would expect to observe dyads from the P1 Asp to the other subsites at P4, P3 and P1'. To test this, equal amounts of caspases-2, -3, -6, -7 and -8 were added separately to the peptide library and samples taken at 5 and 21 hours for analysis. The number of unique Asp-cleaved peptides identified increased with time and ranged from 36 peptides cleaved for caspase-3, to as few as 7 for caspase-2 (Fig. 5A and Dataset S8). The number of observed cuts roughly track

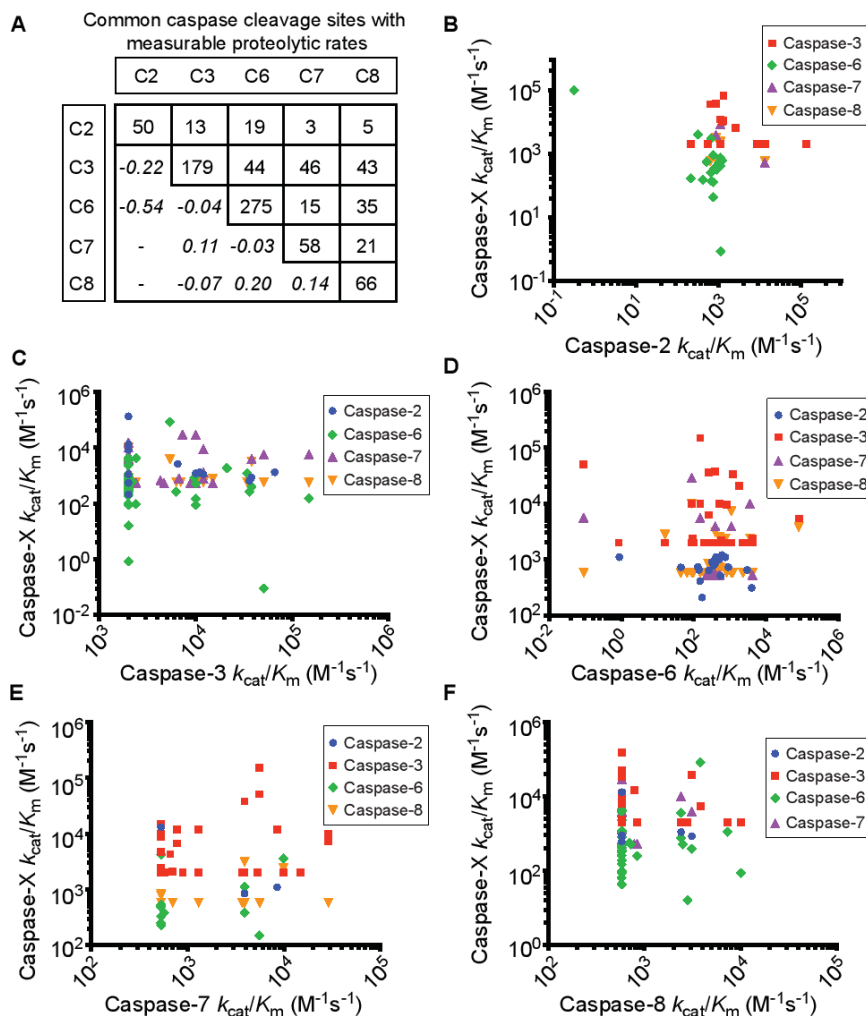


Fig. 4. Pair-wise comparisons of common substrates of caspase-2, -3, -6, -7 and -8 shows uncorrelated catalytic efficiency values. A. Shows the number of common substrates with available rates of proteolysis determined between caspase-2, -3, -6, -7 and -8. B-F. Shows the poor pair-wise comparisons for the rate of proteolysis of the common substrates among the individual caspases. Pearson correlation coefficients are shown in *italic* in A (for $n > 5$). The vertical set of points for caspases-3, -7 and -8 (Panels C, E, and F) reflect the lower limit of detection for slow substrates (10).

previous kinetic experiments on optimized substrates showing that caspase-3 is the most active followed by caspase-8, -7, -6 and -2.

Although the number of cleavage events was far less than those sampled in the N-terminomics experiments, recognition motifs were evident that are similar to the N-terminomics data (Fig. 4B-4F). All show an enrichment for aspartate at P1 and small amino acids at P1'. The consensus (E/V)XAD↓G for caspase-2, VEVD↓G for caspase-6, and (N/E)(L/E)VD↓G for caspases-3, -7 and -8 are not dissimilar from the respective consensus sequences derived from the N-terminomics data shown for caspase-2 and -6 in Fig. 2C, 2D, and previously reported for caspases-3, -7 and -8 (10). The greatest divergence is at P4 between the peptide and protein data but is most likely due to the limited number of peptide sequences present in the peptide library. In fact, DEVD or similar motifs are not in the peptide library, since the library was designed with a focus on pairwise diversity.

We next wished to quantitatively study the different rates of cleavage toward protein and peptide substrate sites to determine to what extent cleavage rates depended on the primary versus tertiary context. For example, it has been previously reported that a tetrapeptide substrate for caspase-1 is cleaved with similar efficiency to a protein substrate (pro-IL1 β) containing the same cleavage site (28). Similarly, we determined the catalytic efficiencies for cleavage of a linear peptide from at least one representative protein substrate identified in the N-terminomics

experiment with fast, medium and slow protein substrate catalytic efficiencies observed for each of the five caspases. We designed tetra-decapeptides corresponding to the P5 to P4' site residues of the protein substrate. At the C-terminus of these peptides, we included a five-residue linker (GGSRR) containing the Arg-Arg sequence that would facilitate efficient ionization thus increasing the sensitivity for the LC-MS/MS measurement. We used SRM to monitor the proteolysis of each peptide over time for each of the five caspases (see Materials and Methods for more details). As above, we performed automated non-linear fitting to determine the rate constant (k_{cat}/K_M) of each caspase toward its peptide substrates (Fig. 6A-6E). Remarkably, in most cases the k_{cat}/K_M values for the cleavages were within a factor of two between linear peptide and intact protein substrates. There were a few notable exceptions for caspase-6 and -8, where the protein substrates were two- to four-fold more active. Previous structural studies on caspase-2 showed that it also can bind to the P5 residue, and our N-terminomics data support this as well (Fig S3). To test this at the primary sequence level we made a peptide lacking a P5 residue in the consensus motif (DEVD↓GLGVAGGSRR) (Fig. 6F). Caspases-3 and -7 cleaved this very rapidly ($k_{cat}/K_M > 10^4$), but caspase-2 was 10-fold reduced from cleaving the KDEVD peptide, which extends to P5 (Fig. 6A) ($k_{cat}/K_M < 10^2$). These data corroborate the proteomics and structural data suggesting the substrate recognition sequence extends to the P5 position for caspase-2.

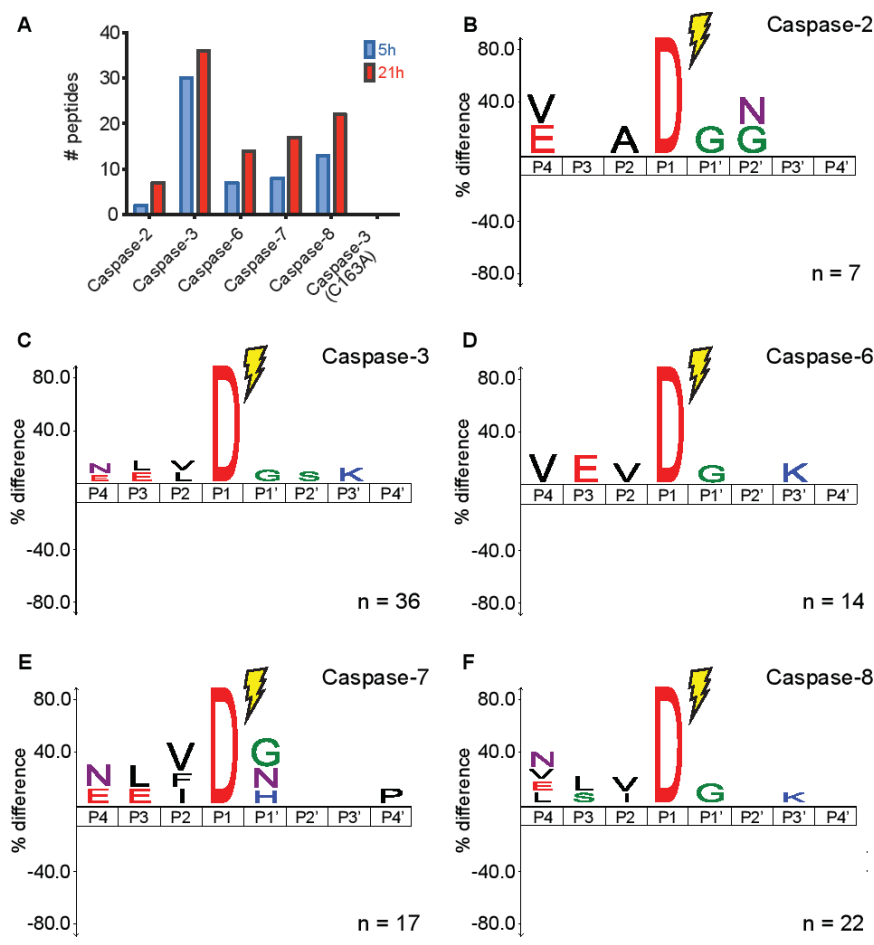


Fig. 5. Caspase-2, -3, -6, -7 and -8 sequence specificity obtained by MSP-MS. Each caspase was incubated with a 228-member degenerate peptide library with the MSP-MS method to evaluate the protease specificity *in vitro* (27). **A.** Total number of peptides cleaved by each enzyme (presence of aspartate at C-termini) after 5 and 24 hours incubation. **B-F.** Sequence recognition motifs of caspase-2, -3, -6, -7 and -8, respectively (P value = 0.05).

Discussion

Importance of sequence and structure in guiding specificity in caspases. Our data support the view that both sequence and structure determine where a protein is cut. We find caspases-2 and -6 cut their substrates on average 1.2-1.3 times per protein, similar to the average number of cuts per substrate protein seen previously for caspase-3, -7 and -8 (10) and observed globally in apoptosis (17, 29). Less than 1/250 of aspartic acids are cleavage sites clearly showing that extended sequence is critical (8, 30). Moreover, using structural bioinformatics for sites of known or modeled proteins, we find that caspase-2 and -6 have similar secondary structural preferences for cutting loops>helices>sheets (SI Appendix, Fig. S8). The same pattern was seen globally during apoptosis (17). It is not surprising that protein structure should play a role since substrates are seen to bind over an eight residue stretch in the active sites of the proteases (31, 32), which requires unfolding of the cut site in the protein. In future studies, one could compare the proteolytic rates in a native cell lysate to those in a fully denatured or partially pre-digested cell lysate.

On the other hand, we see many instances where different caspases cut the same protein at exactly the same site, but at radically different rates. This must reflect the intrinsic specificity of each caspase and not the structural plasticity of the substrate protein. We find the consensus substrate patterns derived from cutting a naive synthetic peptide library using MSP-MS or from natural proteins using subtiligase N-terminomics are similar suggesting differences in the intrinsic specificity of the caspases and not the substrate scaffold. This is remarkable given the methods are totally orthogonal and neither substrate sets have identical

sequences from which consensus patterns are derived. Perhaps most striking is that the differences in rates of cleavage for intact protein substrates compared to their matched synthetic peptides for each of the five caspases are generally small, within a factor of two to four. Caspase-7 has been shown to have a highly charged exosite region distant from the active site that imparts a 30-fold advantage to cleaving the protein, PARP-1 (33). Although our data could suggest some exosite component to account for more rapid cleavage of the protein substrate compared to the corresponding peptide substrate, the rate differences are small and could be due to differences in the kinetic methods employed for the protein and peptide substrates.

The use of structural information (secondary structure, solvent accessibility, degrees of disordered regions), in combination with the primary sequence of validated apoptotic substrates, has been previously used to predict caspase cleavage sites (30). In these studies, all possible caspase cleavage sites in the human proteome were ranked based on their support vector machine (SVM) score, representing the likelihood of a given site to be a "real" caspase cleavage site. This generated 5×10^6 predictions of all octapeptides showing an aspartate at P1. We extracted the SVM score for each caspase-2 and -6 cleavage site from this dataset and compared it to the overall predictions. This analysis showed an average SVM score of 0.54 for the caspase-2 cleavage sites observed in our studies, while the average SVM score for all predicted sites is only -1.99 (Gaussian distribution ranging from -6 to 4) (SI Appendix, Fig. S9 and Fig. S10). Similarly, we obtained an average SVM score of 0.26 for caspase-6. These data further validate the methodology used by Barkan et al. to predict

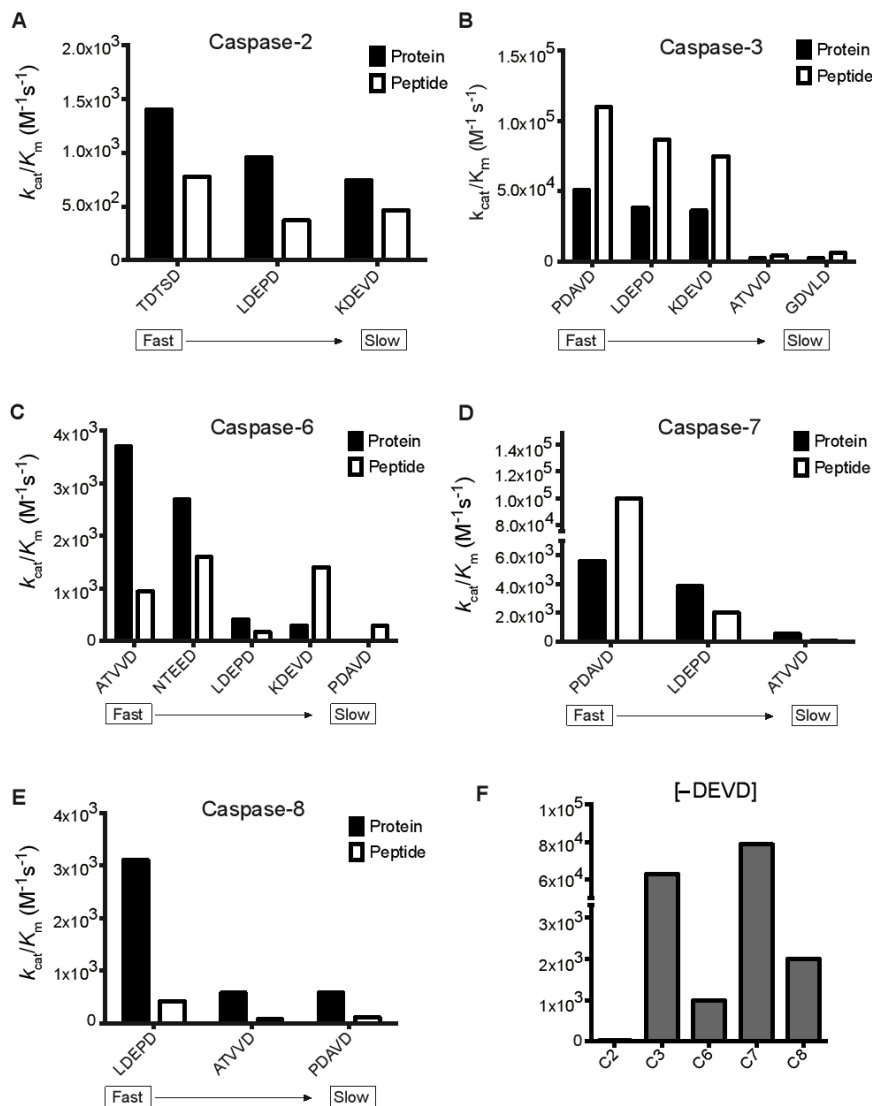


Fig. 6. Rates of proteolysis for protein substrates compared to their corresponding peptide sequences. A-E. Proteolysis rate constants for fast, medium, and slow substrates of caspase-2, -3, -6, -7 and -8, and corresponding tetradecapeptide sequences. P5-P1 residue sequences that match the corresponding protein cut sites are shown on the X-axis. F. Cleavage rate constants for a DEVD+GLGVAGGSRR peptide, lacking a P5 residue, highlighting the importance of this residue for caspase-2.

caspase cleavage sites, exploiting both the primary sequence and structural features of the substrates. It is possible these predictive models could be improved for the specific caspases, if they utilized training sets based on the catalytic efficiencies for individual substrates for each of the caspases generated here, instead of a more generic motif derived from apoptosis data that likely emphasizes caspase-3, -7 and -8 cleavage sites.

Dissecting functional differences among caspase family members. Our studies highlight tools and results that allow greater distinction among caspases in their specificity, cellular substrates, and cell biology. The N-terminomics discovery approach provided reproducible lists of hundreds of natural proteins cleaved by exogenously added caspases-2 and -6. Although it is possible that some of these cleavages are derived indirectly from activation of other procaspases in the neutralized extract, we believe this is unlikely for the vast majority of substrates. First, there are many unique substrates for caspases-2 and -6 that do not overlap, and for this massive difference to result from secondary activation would require down-stream activation of different procaspases for caspase-2 and -6 with unique specificity. Second, there are a number of common substrates, cleaved at the same site but at very different rates, which again would require activation of a unique procaspase for each substrate. The progress

curves for the SRM analysis of >300 substrates for caspases-2 and -6 show no lag phase, which would be expected for a cascade activation event. Furthermore, the substrate cleavage sequence patterns determined from N-terminomics for the caspases-2 and -6 differed from each other and were mirrored in the MSP-MS data. The rates of cleavage were similar for the N-terminomics extract and synthetic peptide data.

GO analysis provides some clues to help organize the cellular logic for cleaving these client proteins. Caspase-2 cleaves proteins involved in RNA processing, and caspase-6 cleaves proteins involved in cell cycle, DNA damage and splicing. Both have strong components involving cytoskeleton and cell death, which we have seen in apoptotic datasets (17). Importantly, we believe that the identified substrates are a valuable resource for understanding caspase biology, and the identification of these specific targets could further our understanding of their respective biological function. We find caspase substrates identified to belong to three different categories. First, we identified many new substrates of caspases-2 and -6, and report 128 (out of 235) and 553 (out of 871) new caspase substrates that have not been previously reported in our apoptotic database of caspase substrates (out of 1268) (8). Second, we identified many known substrates but in many instances the exact location was not known until our studies here.

For example, we could confirm cleavage of BNIP-2 by caspase-6 at IDLD₈₃GLDT, as speculated in previous studies (34). Finally, there are substrates for which the cleavage site is known, but the enzyme that catalyzes the cleavage was until now unknown, and in fact we can deorphan that cleavage. For example, we found that the previously unidentified caspase substrate tuberous sclerosis (TSC1), also called hamartin, is cleaved by caspase-6 at position 638 (TEED₆₃₈). This substrate has been seen many times in our apoptotic datasets (8), confirming its biological importance, but the identity of the protease remained unknown until now. Hamartin has been shown to confer protection in CA3 hippocampal neurons from the effects of stroke (35). Also consistent with the conjecture in the literature that caspase-6 plays a role in neurons, we identified the substrate PARK7, a peptidase involved in Parkinson's disease from which an N-terminal fragment was shown to promote apoptosis via increased ROS production (36). We also identified superoxide dismutase (SODC, or SOD1) as a caspase-6 substrate, an important protein capable of misfolding and forming aggregates that leads to amyotrophic lateral sclerosis (ALS, or Lou Gehrig's disease). The use of different cell lines, such as a neuronal cell line to study the specific involvement of caspase-6 in neurodegeneration, should help to clarify caspase biology in specific tissues.

Of the tools we have employed to distinguish the functions of caspases, SRM analysis appears to be the most comprehensive. From a technical point of view, it provides multiple point confirmation that a protein is cleaved. In the substrate discovery phase, biological replicates provide some confidence that the method is reproducible; however, the seven-point kinetic analysis improves the confidence level in determining which proteins are truly cleaved. SRM provides an estimation of catalytic efficiencies for natural caspase substrates (Dataset S7) and can reveal that the rates of cleavage for the same site can differ by over 100-fold for each enzyme. This strongly supports a view that each caspase likely plays a unique and non-redundant role, and opens a window into understanding the catalytic cascade orchestrated by multiple caspases.

Although it is not in the scope of this paper to functionally annotate the individual roles of these cleaved substrates in driving caspase biology, we would hope these data will inspire the community to pursue detailed studies on individual substrates. For example, previous proteomic data showed gasdermin D is uniquely cut by caspase-1, but not the other inflammatory caspases-4 or -5 in cell extracts (9). Recently, two labs have shown that gasdermin-D is a key mediator in the biology of caspase-1 (37, 38). To facilitate further the analysis of the data here, we show a Venn diagram for the unique and overlapping substrates for which we have SRM data (SI Appendix, Fig. S12). The vast majorities are unique to individual caspases, but some are surprisingly promiscuous. In our SRM dataset, 11 substrates are cleaved by four or five caspases, and one is cleaved by all, DGCR8. DGCR8 complexes the Drosha enzyme and is essential for microRNA processing (39). Broadly, these studies highlight the value of determining both site specificity and kinetic activity for substrates within the context of natural proteins and linear peptides to understand how substrate sequence and structure can functionally distinguish family members involved in post-translational modifications.

Material and methods

Cloning and Recombinant Protein Expression and Purification. Caspase-2 and -6 were cloned into His₆-affinity tag containing vector pET23b (Novagen). The active enzymes were expressed in *E. Coli* BL21 (DE3) pLysS cells (Stratagene). Cells were grown in 2xYT media supplemented with 200 µg/ml ampicillin at 37°C to an OD_{600nm} at approximately ~0.6-0.8. Caspase overexpression was induced with 0.2 mM IPTG at 16°C overnight. Cells were harvested by centrifugation and lysed by microfluidization (Microfluidics). The cell lysates were clarified

by centrifugation and the soluble fractions were purified by Ni-NTA superflow resin (Millipore). His-tagged caspase was then loaded on mono Q ion exchange column for further purification. Peak fractions were combined, concentrated, and stored at -80°C.

N-Terminal Labeling and Enrichment. For each discovery replicate, 1x10⁹ Jurkat cells were harvested by centrifugation and lysed (0.1% Triton x-100) in the presence of protease inhibitors (5 mM EDTA, 1 mM AEBSE, 1 mM PMSF, 10 mM IAM). Excess cysteine-protease inhibitors were neutralized with 20 mM DTT, and caspase buffer was added (20 mM HEPES, 50 mM NaCl, 15 mM MgCl₂ and 1.5% sucrose, 10mM DTT) prior to addition of 500 nM of exogenous caspase-2 or caspase-6 for up to four hours. As a function of time, the exogenous caspase activity was then neutralized with 100 uM zVAD-fmk. N-terminal labeling was then performed with 1 uM subtiligase and 1 mM TEVTest4B (Fig. S2) for two hours. Tagged protein fragments were precipitated using acetonitrile, then denatured (8 M Gdn-HCl), reduced (2 mM TECP) and thiols alkylated (4 mM IAM), before ethanol precipitation. Biotinylated N-terminal peptides were then captured with neutravidin agarose beads for 48 hours. The beads were washed using 4 M Gdn-HCl, trypsinized, and released from the beads using TEV protease. The tryptic peptides fractionated into 15 fractions/sample using high pH reverse phase C₁₈ chromatography, and were then desalted with a C₁₈ ZipTip (Millipore).

Discovery Mass Spectrometry. LC-MS/MS was carried out by reverse phase LC interfaced with a LTQ Orbitrap Velos (ThermoFisher Scientific) mass spectrometer. A nanoflow HPLC (NanoAcquity UPLC system, Waters Corporation) was equipped with a trap column (180 µm X 20 mm, 5 µm SymmetryC₁₈, from Waters) and an analytical column (100 µm X 100 mm, 1.7 µm BEH130C₁₈, from Waters). Peptides were eluted over a linear gradient over 60 min from 2% to 30% acetonitrile in 0.1% formic acid. MS and MS/MS spectra were acquired in a data-dependent mode with up to six HCD MS/MS spectra acquired for the most intense parent ions per MS. For data analysis, peptide sequences were assigned using the ProteinProspector (v5.10.15) database search engine (<http://prospector.ucsf.edu/prospector/mshome.htm>) against the Swiss-Prot human protein database (2013.6.27). Search parameters included a precursor mass tolerance of 20 ppm, fragment ion mass tolerance of 20 ppm, up to two missed trypsin cleavages, constant carbamidomethylation of Cys, variable modifications of N terminal addition of Abu amino acid, acetylation of protein N terminus, and oxidation of methionine. The identified peptides were searched against a random decoy protein database for evaluating the false positive rates. The false discovery rate never exceeded 1.3% at the maximum expectation value of peptide set at 0.05.

Selected Reaction Monitoring (SRM) method development. The caspase peptides (P1=D) observed in the caspase-2 and -6 datasets where imported into SkyLine (v2.5.0) (40) in order to build a scheduled SRM method. For each peptide, based on the spectral library generated from our discovery dataset above, we selected the seven most intense parent ion-fragment ion transitions (y- and b-series ions only). The retention times observed for each peptide during the discovery experiments were used for this initial method with a window of 15 min. A small portion of the discovery samples was reserved to develop the SRM method. These peptides were injected on an AB Sciex QTRAP 5500 triple quadrupole mass spectrometer interfaced in-line with a nanoAcquity UPLC system (Waters) identical to that on the LTQ Orbitrap Velos (Trapping column: Symmetry C18 Column (0.18 • 20 mm, 5 µm; Waters); Analytical column: BEH130 C18 column (0.075 • 200 mm column, 1.7 µm; Waters)). The SRM data obtained was imported into SkyLine for analysis. Positive peptide identification by SRM was based on (i) detection of at

least four co-eluting targeted transitions above baseline noise, (ii) retention time within ± 5 min of that obtained in the discovery dataset, and (iii) relative intensity of fragment ions similar to that found in discovery spectral library. Each peptide detected from the caspase-2 and -6 datasets was manually analyzed, and four transitions (out of seven) were selected for further method refinement. The preferred transitions were defined as the most intense peaks, least noise or background interference, and higher m/z within the monitored window between 300 and 1250 Da. Ultimately, our final SRM method included 152 and 471 peptides (plus two controls each) for caspase-2 and -6, respectively. This new scheduled SRM method was developed with a retention time window of ± 5 min and used for each time point sampled below.

SRM acquisition, time course and data analysis. The subtiligase N-terminomics enrichment method described above was used to monitor the appearance of cleaved products as a function of time, with 2×10^9 and 4×10^9 Jurkat cells for caspase-2 and -6, respectively. For each sample, an aliquot was taken out after 0, 5, 15, 30, 60, 120 and 240 min incubation with 500 nM exogenous protease and quenched with 100 μ M zVAD-fmk. Samples were processed for data acquisition on the QTrap 5500 with one and two injections per sample for caspase-2 and -6, respectively. The SRM data for each sample was imported into Skyline for quantification. The sum of the peak area of the 4 transitions for each peptide was measured as a function of time. The global mean of the control peptides for each time point was used to normalize each summation. Non-linear fitting was performed using Grace (<http://plasma-gate.weizmann.ac.il/Grace/>) using pseudo-first order kinetics: $Y = Y_{max} (1 - e^{-k_{cat}t})$, where Y is the sum of the peak area, Y_{max} is the peak area at maximal value, t is the time of incubation, and k is the observed rate of proteolysis (k_{cat}/K_M) multiplied by the enzyme concentration (E_0).

Peptide cleavage site identification by multiplex substrate profiling-mass spectrometry. Intrinsic substrate specificity was determined with the MSP-MS method (27) with modifications as reported (41). Briefly, 228 tetra-decapeptides were split in two pools of 114 peptides each (500 nM) in assay buffer (20 mM HEPES, 50 mM NaCl, 15 mM Mg_2Cl and 1.5% sucrose, 10 mM DTT), to which was added caspase-2 or caspase-6 (both at 200 nM final concentration), or an equal volume of buffer as a no-enzyme

control in a final reaction volume of 150 μ l for each reaction. Samples were incubated at room temperature (19–22°C), 30 μ l aliquots were removed at 15, 60, 300 and 1260 min, and quenched with formic acid to a final concentration of 0.4% v/v. Samples were desalted by C18 ZipTip (Millipore), then lyophilized and stored at $-80^\circ C$. Peptides were sequenced by LC-MS/MS on an LTQ-OrbitrapXL (Thermo) mass spectrometer equipped with a nanoAcquity UPLC system (Waters) using identical methods to those reported (41). Data were processed and searched as reported (41).

Rate of proteolysis of tetra-decapeptides peptides determined by quantitative mass spectrometry. To compare the catalytic efficiency of the caspases against synthetic peptides versus intact protein measurements, a peptide library was designed by selecting a set of fast, medium, and slow substrates for each studied caspase, in order to manage the number of peptides required. Peptides were obtained from GenScript inc. and Shengnuo inc. (see Dataset S8). The peptide library (4 μ M) was added to caspase buffer (20 mM HEPES, 50 mM NaCl, 15 mM $MgCl_2$ and 1.5% sucrose, 10 mM DTT) prior to addition of a given caspase at 500 nM. For each sample, an aliquot was taken out after 0, 5m, 15m, 30m, 60m, 120m, 240m, 360m and 24h incubation and quenched with 100 μ M zVAD-fmk. Samples were processed as mentioned above, and data was acquired on a QExactive Plus (Thermo) using parallel reaction monitoring mode. The data was imported into Skyline for quantification, as described above for protein substrates.

Acknowledgements.

We thank Justin Rettenmaier, Zachary Hill, Amy Weeks, Matthew Ravalin, Rebecca Levin, Julia Seaman and Nicholas Agard for helpful discussions and technical help. We are grateful to Julie Zorn, Yinyan Tang and Dongju Wang for providing caspases. Mass spectrometry was performed at the Bio-Organic Biomedical Mass Spectrometry Resource at University of California at San Francisco (Alma Burlingame, Director), supported by Biomedical Research Technology Program of the National Institutes of Health National Center for Research Resources (Grants P41RR001614 and 1S10RR026662) and the Howard Hughes Medical Institute. A.P.W. is supported by the Damon Runyon Cancer Research Foundation (DRG 11-112 and Df5 16-15). This project was supported in part by Grants from National Institutes of Health R21 CA186007 (C.S.C.), R01 GM081051, R01 GM097316, and R01 CA154802 (J. A. W.); O.J. is the recipient of a Banting Postdoctoral Fellowship funded by the Canadian Institutes of Health Research and the Government of Canada, and a fellowship from the UCSF Program for Breakthrough Biomedical Research, which is funded in part by the Sandler Foundation.

- Thornberry NA, Lazebnik Y (1998) Caspases: enemies within. *Science* 281(5381):1312–1316.
- Yuan J, Kroemer G (2010) Alternative cell death mechanisms in development and beyond. *Genes Dev* 24(23):2592–2602.
- Crawford ED, Wells JA (2011) Caspase substrates and cellular remodeling. *Annu Rev Biochem* 80:1055–1087.
- Lamkanfi M, Declercq W, Kalai M, Saelens X, Vandenabeele P (2002) Alice in caspase land. A phylogenetic analysis of caspases from worm to man. *Cell Death Differ* 9(4):358–361.
- Salvesen GS, Ashkenazi A (2011) Snapshot: caspases. *Cell* 147(2):476–476.e1.
- Dix MM, Simon GM, Cravatt BF (2014) Global identification of caspase substrates using PROTOMAP (protein topography and migration analysis platform). *Methods Mol Biol* 1133:61–70.
- Staes A, Impens F, Van Damme P, Rutters B, Goethals M *et al.* (2011) Selecting protein N-terminal peptides by combined fractional diagonal chromatography. *Nat Protoc* 6(8):1130–1141.
- Crawford ED, Seaman JE, Agard N, Hsu GW, Julien O *et al.* (2013) The DegraBase: a database of proteolysis in healthy and apoptotic human cells. *Mol Cell Proteomics* 12(3):813–824.
- Agard NJ, Maltby D, Wells JA (2010) Inflammatory stimuli regulate caspase substrate profiles. *Mol Cell Proteomics* 9(5):880–893.
- Agard NJ, Mahrus S, Trinidad JC, Lynn A, Burlingame AL *et al.* (2012) Global kinetic analysis of proteolysis via quantitative targeted proteomics. *Proc Natl Acad Sci USA* 109(6):1913–1918.
- Wejda M, Impens F, Takahashi N, Van Damme P, Gevaert K *et al.* (2012) Degradomics reveals that cleavage specificity profiles of caspase-2 and effector caspases are alike. *J Biol Chem* 287(41):33983–33995.
- Walsh JG, Cullen SP, Sheridan C, Lüthi AU, Gerner C *et al.* (2008) Executioner caspase-3 and caspase-7 are functionally distinct proteases. *Proc Natl Acad Sci USA* 105(35):12815–12819.
- Timmer JC, Zhu W, Pop C, Regan T, Snipas SJ *et al.* (2009) Structural and kinetic determinants of protease substrates. *Nat Struct Mol Biol* 16(10):1101–1108.
- Talanian RV, Quinlan C, Trautz S, Hackett MC, Mankovich JA *et al.* (1997) Substrate specificities of caspase family proteases. *J Biol Chem* 272(15):9677–9682.
- Graham RK, Ehrnhoefer DE, Hayden MR (2011) Caspase-6 and neurodegeneration. *Trends Neurosci* 34(12):646–656.
- Flygare JA, Arkin MR (2014) Inhibiting caspase-6 activation and catalytic activity for neurodegenerative diseases. *Curr Top Med Chem* 14(3):319–325.
- Mahrus S, Trinidad JC, Barkan DT, Sali A, Burlingame AL *et al.* (2008) Global sequencing of proteolytic cleavage sites in apoptosis by specific labeling of protein N termini. *Cell* 134(5):866–876.
- Weiss A, Wiskocil RL, Stobo JD (1984) The role of T3 surface molecules in the activation of human T cells: a two-stimulus requirement for IL 2 production reflects events occurring at a pre-translational level. *J Immunol* 133(1):123–128.
- Arnesen T, Van Damme P, Polevoda B, Helsen K, Evjenth R *et al.* (2009) Proteomics analyses reveal the evolutionary conservation and divergence of N-terminal acetyltransferases from yeast and humans. *Proc Natl Acad Sci USA* 106(20):8157–8162.
- Thornberry NA, Rano TA, Peterson EP, Rasper DM, Timkey T *et al.* (1997) A combinatorial approach defines specificities of members of the caspase family and granzyme B. Functional relationships established for key mediators of apoptosis. *J Biol Chem* 272(29):17907–17911.
- Klaiman G, Petzke TL, Hammond J, Leblanc AC (2008) Targets of caspase-6 activity in human neurons and Alzheimer disease. *Mol Cell Proteomics* 7(8):1541–1555.
- Igarashi Y, Heuvel E, Doctor KS, Talwar P, Gramatikova S *et al.* (2009) PMAP: databases for analyzing proteolytic events and pathways. *Nucleic Acids Res* 37(Database issue):D611–8.
- Colaert N, Helsen K, Martens L, Vandekerckhove J, Gevaert K (2009) Improved visualization of protein consensus sequences by iceLogo. *Nat Methods* 6(11):786–787.
- Stennicke HR, Renatus M, Meldal M, Salvesen GS (2000) Internally quenched fluorescent peptide substrates disclose the subsite preferences of human caspases 1, 3, 6, 7 and 8. *Biochem J* 350 Pt 2:563–568.
- McStay GP, Salvesen GS, Green DR (2008) Overlapping cleavage motif selectivity of caspases: implications for analysis of apoptotic pathways. *Cell Death Differ* 15(2):322–331.
- Zorn JA, Wolan DW, Agard NJ, Wells JA (2012) Fibrils colocalize caspase-3 with procaspase-3 to foster maturation. *J Biol Chem* 287(40):33781–33795.
- O'Donoghue AJ, Eroy-Reveles AA, Knudsen GM, Ingram J, Zhou M *et al.* (2012) Global identification of peptidase specificity by multiplex substrate profiling. *Nat Methods*

1225 9(11):1095–1100.

1226 28. Rano TA, Timkey T, Peterson EP, Rotonda J, Nicholson DW *et al.* (1997) A combinatorial

1227 approach for determining protease specificities: application to interleukin-1beta converting

1228 enzyme (ICE). *Chem Biol* 4(2):149–155.

1229 29. Dix MM, Simon GM, Cravatt BF (2008) Global mapping of the topography and magnitude

1230 of proteolytic events in apoptosis. *Cell* 134(4):679–691.

1231 30. Barkan DT, Hostetter DR, Mahrus S, Pieper U, Wells JA *et al.* (2010) Prediction of protease

1232 substrates using sequence and structure features. *Bioinformatics* 26(14):1714–1722.

1233 31. Chai J, Wu Q, Shiozaki E, Srinivasula SM, Alnemri ES *et al.* (2001) Crystal structure of a

1234 procaspase-7 zymogen: mechanisms of activation and substrate binding. *Cell* 107(3):399–407.

1235 32. Fuentes-Prior P, Salvesen GS (2004) The protein structures that shape caspase activity,

1236 specificity, activation and inhibition. *Biochem J* 384(Pt 2):201–232.

1237 33. Boucher D, Blais V, Denault JB (2012) Caspase-7 uses an exosite to promote poly(ADP

1238 ribose) polymerase 1 proteolysis. *Proc Natl Acad Sci U S A* 109(15):5669–5674.

1239 34. Valencia CA, Cotten SW, Liu R (2007) Cleavage of BNIP-2 and BNIP-XL by caspases.

1240 *Biochem Biophys Res Commun* 364(3):495–501.

1241 35. Papadakis M, Hadley G, Xilouri M, Hoyte LC, Nagel S *et al.* (2013) Tsc1 (hamartin) confers

1242 neuroprotection against ischemia by inducing autophagy. *Nat Med* 19(3):351–357.

36. Robert G, Puissant A, Dufies M, Marchetti S, Jacquel A *et al.* (2012) The caspase 6 derived

37. N-terminal fragment of DJ-1 promotes apoptosis via increased ROS production. *Cell Death Differ* 19(11):1769–1778.

38. Kayagaki N, Stowe IB, Lee BL, O'Rourke K, Anderson K *et al.* (2015) Caspase-11 cleaves

39. gasdermin D for non-canonical inflammasome signalling. *Nature* 526(7575):666–671.

40. Shi J, Zhao Y, Wang K, Shi X, Wang Y *et al.* (2015) Cleavage of GSDMD by inflammatory

41. caspases determines pyroptotic cell death. *Nature* 526(7575):660–665.

42. Han J, Lee Y, Yeom KH, Kim YK, Jin H *et al.* (2004) The Droscha-DGCR8 complex in

43. primary microRNA processing. *Genes Dev* 18(24):3016–3027.

44. MacLean B, Tomazela DM, Shulman N, Chambers M, Finney GL *et al.* (2010) Skyline: an

45. open source document editor for creating and analyzing targeted proteomics experiments. *Bioinformatics* 26(7):966–968.

46. O'Donoghue AJ, Knudsen GM, Beekman C, Perry JA, Johnson AD *et al.* (2015) Destructin-

47. 1 is a collagen-degrading endopeptidase secreted by *Pseudogymnoascus destructans*, the

48. causative agent of white-nose syndrome. *Proc Natl Acad Sci USA* 112(24):7478–7483.

Submission PDF

1293
1294
1295
1296
1297
1298
1299
1300
1301
1302
1303
1304
1305
1306
1307
1308
1309
1310
1311
1312
1313
1314
1315
1316
1317
1318
1319
1320
1321
1322
1323
1324
1325
1326
1327
1328
1329
1330
1331
1332
1333
1334
1335
1336
1337
1338
1339
1340
1341
1342
1343
1344
1345
1346
1347
1348
1349
1350
1351
1352
1353
1354
1355
1356
1357
1358
1359
1360